International Journal of Pharmaceutics 511 (2016) 785–793

Contents lists available at ScienceDirect

International Journal of Pharmaceutics

journal homepage: www.elsevier.com/locate/ijpharm

# Nanoencapsulated budesonide in self-stratified polyurethane-polyurea nanoparticles is highly effective in inducing human tolerogenic dendritic cells

Georgina Flórez-Grau[a,1], Pau Rocas[b,1], Raquel Cabezón[a], Carolina España[c], Julián Panés[a,c], Josep Rocas[d], Fernando Albericio[b,e,f,g,**], Daniel Benítez-Ribas[h,*]

[a] Institut d'Investigacions Biomèdiques August Pi i Sunyer (IDIBAPS), Barcelona, Spain
[b] Institute for Research in Biomedicine (IRB Barcelona), The Barcelona Institute of Science and Technology, Barcelona, Spain
[c] Fundació Clínic per la Recerca Biomèdica, Barcelona, Spain
[d] Nanobiotechnological Polymers Division, Ecopol Tech S.L., Tarragona, Spain
[e] Department of Organic Chemistry, University of Barcelona, Barcelona, Spain
[f] School of Chemistry & Physics, University of Kwazulu-Natal, Durban, South Africa
[g] Networking Centre on Bioengineering Biomaterials and Nanomedicine (CIBER-BBN), Barcelona, Spain
[h] Centro de Investigación Biomédica en Red, Enfermedades Hepáticas y Digestivas (CIBERehd), Barcelona, Spain

ARTICLE INFO

*Article history:*
Received 19 May 2016
Received in revised form 21 July 2016
Accepted 24 July 2016
Available online 28 July 2016

*Keywords:*
Nanoimmunotherapy
Polyurethane-polyurea nanoparticles
Tolerogenic dendritic cells
Multiwalled nanostructures
Budesonide nanoencapsulation
Cell therapies

ABSTRACT

The design of innovative strategies to selectively target cells, such antigen-presenting cells and dendritic cells, *in vivo* to induce immune tolerance is gaining interest and relevance for the treatment of immune-mediated diseases.

A novel loaded-nanosystem strategy to generate tolerogenic dendritic cells (tol-DCs) was evaluated. Hence budesonide (BDS) was encapsulated in multiwalled polyurethane-polyurea nanoparticles (PUUa NPs-BDS) based on self-stratified polymers by hydrophobic interactions at the oil-water interface. DCs treated with encapsulated BDS presented a prominent downregulation of costimulatory molecules (CD80, CD83 and MHCII) and upregulation of inhibitory receptors. Moreover, DCs treated with these PUUa NPs-BDS also secreted large amounts of IL-10, a crucial anti-inflammatory cytokine to induce tolerance, and inhibited T lymphocyte activation in a specific manner compared to those cells generated with free BDS. These results demonstrate that PUUa NPs-BDS are a highly specific and efficient system through which to induce DCs with a tolerogenic profile. Given the capacity of PUUa NPs-BDS, this delivery system has a clear advantage for translation to *in vivo* studies.

© 2016 Elsevier B.V. All rights reserved.

## 1. Introduction

In the last decade, nanoimmunotherapy has emerged as a novel strategy to bolster the capacity of the immune system to counteract different diseases ranging from cancer to immune-mediated diseases (Tacken et al., 2007; De Fuente et al., 2014; Cheung and Mooney, 2015). Several studies have demonstrated the therapeutic potential of manipulating and unleashing our own immune system to tackle cancer or infectious diseases (Kirkwood et al., 2012). Dendritic cells (DCs) are key regulators of the immune response. They are a heterogeneous subset of immune cells recognized as highly potent antigen-presenting cells (APCs) that link innate and adaptive immune responses. DCs are crucial in inducing immunogenic and tolerogenic responses to pathogens or harmless antigens, respectively (Shao et al., 2014; Gharagozloo et al., 2015). DCs are highly specialized in capture and processing

*Abbreviations:* APCs, antigen-presenting cells; Bayhydur 3100, hydrophilic aliphatic polyisocyanate based on hexamethylene diisocyanate (HDI); BDS, budesonide; DCs, dendritic cells; DiI, 1,1′-dioctadecyl-3,3,3′3′-tetramethylindocarbocyanine perchlorate+; IL-, interleukin; MLR, mixed leucocyte reaction; PBMCs, peripheral blood mononuclear cells; PBLs, peripheral blood lymphocytes; PUUa NPs, polyurethane-polyurea nanoparticles; PUUa NPs-BDS, polyurethane-polyurea nanoparticles loaded with Budesonide; PUUa NPs-DiI, polyurethane polyuria nanoparticles loaded with DiI; YMER N-120, linear difunctional polyethylene glycol monomethyl ether; Tol-DCs, tolerogenic dendritic cells; TNFα, tumor necrosis factor α.

* Corresponding author at: Department of Experimental Gastroenterology, CIBERehd, C/ Roselló 149-153, Barcelona 08036, Spain.
** Corresponding author at: Department of Organic Chemistry, University of Barcelona, Barcelona Science Park, Baldiri Reixac 10, Barcelona 08028, Spain.
*E-mail addresses:* albericio@ub.edu (F. Albericio), daniel.benitez@ciberehd.org (D. Benítez-Ribas).
[1] This authors contributed equally to this work.

http://dx.doi.org/10.1016/j.ijpharm.2016.07.056
0378-5173/© 2016 Elsevier B.V. All rights reserved.

antigens in order to convert proteins into small peptides. These peptides are then presented to T-cells by major histocompatibility complexes (MHC) to initiate immune responses (Banchereau and Steinman, 1998; Steinman and Banchereau, 2007). Once immature DCs have recognized pathogens through specialized receptors, they mature to acquire the capacity to stimulate T-cells. The activation and polarization of T-cells is induced through costimulatory molecules, such as CD80, CD83 and CD86, which are upregulated on the mature DC (mDC) membrane, as well as through the secretion of pro- or anti-inflammatory cytokines such as interleukin IL-6, IL-12p70, IL-23 TNF-α or IL-10. The cytokine secretion pattern strongly defines the resulting polarization of T-cells, thereby determining the type of immune response, namely effector Th1, Th2 or Th17 immunity (IL-12p70, IL-23 and TNF-α) or tolerance induction through regulatory T-cells or Tr1 (IL-10) (Collin et al., 2013).

Due to their physiological properties and the availability of clinical grade reagents, immunogenic DCs have been safely and successfully used in clinical trials aiming to generate an efficient immune response against tumors and infectious diseases (Butterfield, 2013; Anguille et al., 2014; Banchereau et al., 2000). Furthermore, as DCs play a key role in maintaining immune tolerance, the generation of tolerogenic DCs (tol-DCs) has great potential in immunotherapy approaches in several immune-mediated diseases such as diabetes, rheumatoid arthritis, multiple sclerosis, and Crohn's disease (Pulendran et al., 2010; Steinman et al., 2003; Cabezón and Benítez-Ribas, 2013; Hu and Wan, 2011; Benham et al., 2015).

Several protocols, including the generation of DCs in the presence of corticosteroids, such as BDS, have been described to produce tol-DCs *in vitro* (Hackstein and Thomson, 2004; Van Kooten et al., 2009). These cells present a semi-mature phenotype, a pronounced shift towards anti-inflammatory versus inflammatory cytokine production and a low capacity to stimulate T-cells. The increased secretion of IL-10 by tol-DCs is considered critical to induce tolerance (Zheng et al., 2013; Cabezón et al., 2012; Kalantari et al., 2011; García-González et al., 2013).

To date, DC-based therapies involve the isolation and *ex vivo* generation of DCs (Jauregui-Amezaga et al., 2015; Suwandi et al., 2016). These approaches require the preparation of individualized autologous cells and thus call for costly culture protocols in certified GMP facilities (Naranjo-Gómez et al., 2011) and standardization of the procedures among laboratories when Phase II or III are planned. An alternative approach to *ex vivo* cell generation is the *in vivo* targeting of specific immune cells in order to manipulate and modulate their function. Several approaches to deliver immunogenic or regulatory agents have been explored, including nanopolymeric systems of PLGA (poly(lactic-*co*-glycolic acid)) and PLLA (poly-L-lactide), and liposomes (Park et al., 2013). Nanoparticle systems improve DC-targeted delivery of tumor antigens, amplify immune activation via the use of immunostimulatory materials, and increase the efficacy of adoptive cell therapies (Amoozgar and Goldberg, 2015; Cho et al., 2011; Fang et al., 2014). Interestingly, the possibility to target DCs *in vivo* paves the way for immunotherapeutic approaches to treat human diseases by modifying immune responses without the need to culture cells. Recent studies have shown that nanoencapsulated corticosteroids in controlled release polymeric systems boost the therapeutic efficiency of the drug, as BDS becomes more water soluble (increased bioavailability) and is released only under the required conditions, thus reducing systemic side effects (Siddique et al., 2015; Leonard et al., 2012; Ali et al., 2014; Beloqui et al., 2013). However, many of these delivery systems show insufficient stability under *in vivo* conditions and limited encapsulation capacity as the drug is prematurely released (Zou et al., 2013). We have recently demonstrated that common approaches based on drug encapsulation with monowalled nanostructures are not stable upon interaction with amphiphilic and hydrophobic cell membrane molecules (*e.g.* phospholipids, cholesterol) (Rocas et al., 2015). Thus, the cargo is non-specifically released from the nanoparticle core, poorly internalized by target cells, and less bioactive (Chen et al., 2008). Hence, we envisaged that a disulfide-rich nanopolymeric system based on hydrophobically stratified polymers creating robust multiwalled nanostructures would be an interesting approach to improve encapsulation stability and maintain in-target redox biodegradation and drug release. However, the effect of these multiwalled nanostructures on human primary DCs remains unknown.

Here we evaluated the performance of our previously described redox-sensitive self-stratified multiwalled nanoparticles (Rocas et al., 2015, 2014) to quantitatively encapsulate various amounts of budesonide (BDS) and analyzed the effects of these particles on primary human monocyte-derived DCs (Fig. 1). In addition, we studied the generation of tol-DCs, comparing encapsulated versus soluble BDS. For this purpose, polyurethane-polyurea nanoparticles (PUUa NPs) carrying BDS were incubated with human monocyte-derived DCs and the toxicity and internalization of these particles were evaluated over time. To validate PUUa NPs as an appropriate carrier for immunosuppressive drugs, we assessed costimulatory molecule expression, cytokine production and the capacity to activate T-cells.

## 2. Material and methods

### 2.1. Materials

YMER N-120 was provided by Perstorp (Perstorp, Sweden) and N-Coco-1,3-propylenediamine (Genamin TAP 100D) by Clariant (Barcelona, Spain). The capric/caprylic triglyceride mixture (Crodamol GTCC) was obtained from Croda (Barcelona, Spain), and

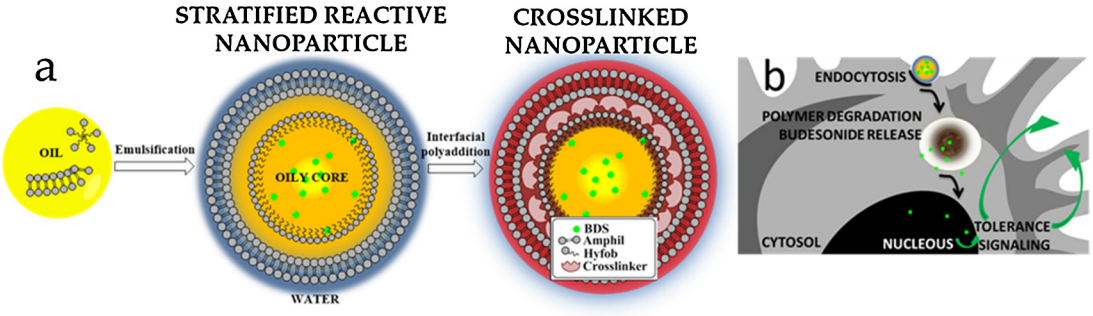


**Fig. 1.** Nanoparticle synthetic strategy and cell internalization. (a) Emulsification of Hyfob and Amphil leads to reactive nanostructures that are further crosslinked in the o/w interface. (b) DC internalization, drug release, and tolerance signaling scheme.

Bayhydur 3100 was purchased from Bayer (Leverkusen, Germany). If not indicated otherwise, all other reagents were purchased from Sigma-Aldrich (St Louis, MO, USA). Extra dry acetone was used during the syntheses.

### 2.2. Experimental methods

#### 2.2.1. Synthesis of reactive prepolymers for multiwalled PUUa NP preparation

The preparation and characterization of the reactive amphiphilic prepolymer (Amphil) and reactive hydrophobic prepolymer (Hyfob) followed previously described methods without modification (Rocas et al., 2015).

*2.2.1.1. Preparation of the reactive amphiphilic prepolymer (Amphil).* A 500-mL four-necked reaction vessel was pre-heated at 50 °C and purged with nitrogen. YMER N-120 (5.50 g, 5.5 mmol), 2-Hydroxyethyl disulfide (DEDS) (0.15 g, 1.0 mmol), Crodamol GTCC (0.75 g), and Isophorone diisocyanate (IPDI) (3.38 g, 15 mmol) were then added to the reaction vessel under mechanical stirring in the presence of dibutyltin dilaurate (DBTL) as catalyst (3 mg, 4.65 μmol). The polyaddition reaction was maintained in these conditions until DEDS and YMER reacted quantitatively with IPDI, as determined by FT-IR and the automatic titration (Clemitson, 2008). At this point, the vessel was cooled to 40 °C, and Genamin TAP 100D (1.45 g, 4.44 mmol) dissolved in 10 g of acetone was added under constant stirring and left to react for 30 min. The formation of polyurethane and polyurethane-polyurea prepolymers was followed by FT-IR and characterized by NMR (Prabhakar et al., 2005).

*2.2.1.2. Preparation of the reactive hydrophobic prepolymer (Hyfob).* To synthesize the hydrophobic prepolymer, a 20-mL Schlenk flask was pre-heated to 50 °C and purged with nitrogen. DEDS (0.15 g, 1.0 mmol) and IPDI (0.485 g, 2.18 mmol) in acetone (7 g) were then added with DBTL as catalyst (0.24 mg, 0.37 μmol) and left to react for 1 h with magnetic stirring. At this point, the Schlenk flask was cooled to 40 °C, and a solution of Genamin TAP 100D (0.15 g, 0.5 mmol) in 3.0 g acetone was added under constant stirring. The reaction was left for 30 min. The formation of polyurethane and polyurethane-polyurea prepolymers was followed by FT-IR and characterized by NMR (Prabhakar et al., 2005).

#### 2.2.2. Synthesis of multiwalled PUUa nanoparticles

*2.2.2.1. Synthesis of PUUa NPs.* A previously homogenized aliquot of Amphil + Hyfob (1.69 g, mass ratio Amphil 13.35:1 Hyfob) (see Section 2.2.1.) was added to a round-bottom flask containing B3100 (125 mg, 0.167 mmol) under nitrogen atmosphere. This organic mixture was then emulsified in pure water (16 mL, 5 °C) in a magnetic stirrer under an ice bath to prevent isocyanate reaction with water. Once the mixture was emulsified, L-lysine was added (68.56 mg, 0.47 mmol). The interfacial polyaddition reaction was controlled by FT-IR. After 30 min, DETA (32.18 mg, 0.31 mmol) was added, and the crosslinked nanoparticles were formed by a second interfacial polyaddition, as shown by FT-IR. Acetone was removed gently under reduced pressure. PUUa NPs were dialysed (100000 MWCO, Spectrum Laboratories, California, USA) against pure water during 72 h for Zeta potential experiments to eliminate salts and traces of monomers. For *in vitro* experiments, PUUa NPs were dialysed against PBS for 72 h to maintain isotonic conditions.

*2.2.2.2. Synthesis of PUUa DiI-loaded NPs (PUUa NPs-DiI).* These NPs were synthesized as previously described (see Section 2.2.2.1.) adding Amphil + Hyfob in a round-bottom flask containing DiI (2.5 mg, 2.67 μmol) as lipophilic fluorophore. The organic mixture was homogenized and, subsequently, Section 2.2.2.1 was followed without modifications.

*2.2.2.3. Synthesis of PUUa Oregon Green 488 Cadaverine-conjugated NPs (PUUa NPs-cad).* An aliquot of this Amphil + Hyfob mixture (0.87 g, mass ratio Amphil 13.35:1 Hyfob) was homogenized in another round-bottom flask with the amine reactive fluorophore Oregon Green 488 Cadaverine (3.2 mg, 6.47 μmol) and B3100 (62 mg, 0.084 mmol). The amino-reactive Oregon Green 488 Cadaverine was left to react for 30 min with excess isocyanate-reactive species at 5 °C under a nitrogen atmosphere and magnetic stirring (273 mg of polymer/mg of dye). At this point, the prepolymers were emulsified in water (8 mL, 5 °C), and L-lysine was added (34.2 mg, 0.24 mmol) to the solution. The interfacial polyaddition reaction was followed by FT-IR. After 30 min, DETA (16.1 mg, 0.16 mmol) was added, and the crosslinked nanoparticles were formed by a second interfacial polyaddition, as shown by FT-IR. Acetone was removed gently under reduced pressure.

*2.2.2.4. Synthesis of 0.5% (w/w) BDS-loaded PUUa NPs (PUUa NPs-BDS 0.5%).* These PUUa NPs were synthesized as previously described (see Section 2.2.2.1.) using BDS as encapsulated molecule. The polymeric organic mixture was homogenized with BDS (10 mg, 23.22 μmol), followed by emulsification in PBS (16 mL, 5 °C) in a magnetic stirrer under an ice bath to prevent isocyanate reaction with water. At this point, Section 2.2.2.1. was followed without further modifications.

*2.2.2.5. Synthesis of 10% (w/w) BDS-loaded PUUa NPs (PUUa NPs-BDS 10%).* These PUUa NPs were synthesized as previously described (see Section 2.2.2.1.) using BDS as encapsulated molecule. The polymeric organic mixture was homogenized with BDS (200 mg, 0.46 mmol), followed by emulsification in PBS (16 mL, 5 °C) in a magnetic stirrer under an ice bath to prevent isocyanate reaction with water. At this point, Section 2.2.2.1. was followed without further modifications.

### 2.3. Analytical techniques

#### 2.3.1. Transmission electron microscopy

Nanoparticle morphology was studied in a Jeol JEM 1010 (Peabody, MA, USA). A 200 mesh copper grid coated with 0.75% FORMVAR was deposited on a drop of 10 mg/mL of nanoparticles in water for 1 min. Excess nanoparticles were removed by washing in fresh MilliQ water for 1 min. The grid was then deposited on a drop of uranyl acetate 2% *w/w* in water for 30 s. Excess uranyl acetate was blotted off, and the grid was air-dried before measurement.

#### 2.3.2. BDS drug loading (DL) and encapsulation efficiency (EE)

To quantify the total amount of encapsulated BDS in PUUa NPs, a calibration curve was performed by preparing standard solutions of BDS in EtOH:H2O (1:1 v/v) for HPLC analysis. Lyophilized PUUa NPs-BDS 0.5% (*w/w*, 5 mg) or PUUa NPs-BDS 10% (*w/w*, 250 μg) (to maintain the same final BDS concentration) were swelled in EtOH: H2O (1:1 v/v) for one week at room temperature (RT) to fully solubilize the drug and then placed in a centrifugal 3 KDa filter unit (Microcon, Carrigtwohill, Ireland) and centrifuged at 14000 *g* for 60 min. Analytical HPLC runs of the filtrate were performed in triplicate in a WATERS 2998 HPLC using a X-Bridge BEH130, C18, 3.5 μm, 4.6 × 100-mm reverse-phase column with the following gradient: 5–100% of B in 8 min at a flow rate of 1 mL/min; eluent A: H2O with 0.045% TFA (v/v); eluent B: CH3CN with 0.036% TFA (v/v) and UV detection at 220 nm. Limit of detection and limit of quantification were set at 0.15 μg/mL and 1.85 μg/mL, respectively.

*2.3.3. Size distribution by DLS*

0.5% PUUa NPs and 10% PUUa NPs were analyzed on a Malvern Zetasizer Nano-ZS90 (Malvern, UK) by diluting them at 1 mg/mL PUUa NPs concentration in pure water at 37 °C.

*2.3.4. Lyophilization and redispersion procedures*

Previously dialyzed samples at a concentration of 100 mg/mL of PUUa NP were lyophilized and directly redispersed at the desired concentration by overnight stirring at 1500 rpm. They were then immediately examined by TEM and DLS to ratify optimal size and morphology characteristics.

*2.4. Biological studies*

*2.4.1. Generation of human DCs*

Peripheral blood mononuclear cells (PBMCs) were isolated from whole blood of healthy donors after Ficoll separation and cultured for 2 h at 37 °C to allow them adhere to the flask. Non-adherent cells, namely Peripheral Blood Lymphocytes (PBLs), were washed and cryopreserved. Monocytes adhered to the flask were cultured in X-VIVO 15 medium (BioWhittaker, Lonza, Belgium) supplemented with 2% AB human serum (Sigma-Aldrich, Spain), IL-4 (300 U/ml), and GM-CSF (450 U/ml) (both from Miltenyi Biotec, Madrid, Spain) for 6 days to obtain immature DCs (iDCs). Maturation cocktail (MC) consisting of IL-1β, IL-6 (both at 1000 U/ml) TNF-α (500 U/ml) (CellGenix, Freiburg, Germany) and $PGE_2$ (10 μg/ml) (Sigma-Aldrich, Spain) was added on day 6 and left for 24 h. To generate tol-DCs, BDS ($10^{-6}$ M) (AstraZeneca Farmaceutica, Spain) was added at day 3. Nanoparticles with BDS (PUUa NPs-BDS 0.05, 0.1 and 1 μM) and empty nanoparticles control (PUUa NPs) were also added at day 3 to compare their effect with those carrying soluble BDS.

For DC stimulation, 100 ng/ml of LPS (Sigma-Aldrich, Spain) was added at day 7 and incubated for 24 h. After stimulation, DC supernatant was collected for cytokine detection.

*2.4.2. Flow cytometry analysis*

In order to evaluate the DC phenotype, flow cytometry was performed. Monoclonal antibodies (mAbs) or their appropriate isotype control were used: Anti-CD80, CD83 and MHCII PE-labeled (BD-pharmigen) and anti-hMer APC-labeled (R&D systems). Flow cytometry was performed using FACSCanto II, and data were analyzed with BD FACSdiva 6.1™ software.

To confirm PUUa NP internalization by DCs, DiI-fluorescently labeled NPs, (NPs-DiI) were added to iDCs and incubated for 10, 30 or 120 min at 37 °C. iDCs positive for DiI-NPs were measured and quantified by flow cytometry (BD LSRFortessa™ cell analyzer).

*2.4.3. Fluorescence microscopy*

In order to confirm NP internalization by DCs, cells were incubated with PUUa DiI-loaded NPs for 120 min, and then washed, fixed, stained with MHC II-FITC, and adhered to a cover slip previously treated with poly L-lysine (Sigma-Aldrich, Spain). Images were obtained with a fluorescence microscope Olympus BX51.

*2.4.4. T-cell proliferation*

A mixed lymphocyte reaction (MLR) was used to test the immunogenicity of DCs. DCs were co-cultured with T-cells from a different donor (standard method in immunology to evaluate DC immunogenicity, the principle is based on the recognition of allogenic MHC class II) at a ratio of 1:20 ($10^5$ T-cells) in 96-round-bottom-well plates. T-cell proliferation was measured using tritrated thymidine (1 μCi/well, Amersham, UK), which was added at day 6. tritrated thymidine incorporation was measured after 16 h. Supernatant was collected at day 6 for IFN-γ analysis.

*2.4.5. Cytokine production*

IL-10, IL-12p70 and IL-23 production by DCs was analyzed by ELISA (eBioscience), following the manufacturer's guidelines. Supernatant from T-cell cultures was collected after 6 days of allogeneic response, and IFN-γ (eBioscience) was analyzed by ELISA following the manufacturer's guidelines.

*2.4.6. Statistical analysis*

Results are shown as the mean ± SD. To determine statistical differences between the means, the paired or independent sample ANOVA test was used., after applying the Kolmogorov-Smirnov test with $p > 0.05$. Bonferroni *post-hoc* test was applied to determine differences between two data sets. Statistical significant differences were set at 0.05. Results are presented as $p < 0.05$ (*), $p < 0.01$(**) or $p < 0.001$(***).

## 3. Results

*3.1. PUUa NP characterization*

Multiwalled PUUa NPs have been extensively characterized in a previous proof-of-principle study (Rocas et al., 2015). In that study, PDI value was obtained as mandated in ISO standards for PDI calculations from DLS measurements PUUa NPs were found to be monodisperse (PDI < 0.1), with a size of 24.4 ± 6.1 nm (PDI = 0.06) and PUUa NPs-BDS 0.5% showed a slight size increase of 28.2 ± 8.1 nm (PDI = 0.08) due to a probable interaction of BDS with self-assembling polymers (Fig. 2). Our system allowed almost 100% of encapsulation efficiency at a drug loading of 5.2 μg BDS per mg PUUa NPs. BDS encapsulation at 0.5% (*w/w*) did not significantly affect the size distribution of nanoparticles. However, a slight increase of 3.8 ± SD was observed for the 0.5% BDS-loaded nanosystem, which may be attributable to minimal hydrophobic interactions of the drug with the stratified prepolymers during NP emulsification. Of note, the morphology of 10% BDS-loaded PUUa NPs, which contained 106 μg BDS per mg PUUa NPs, changed as the core mass was increased 20 times. The higher BDS content

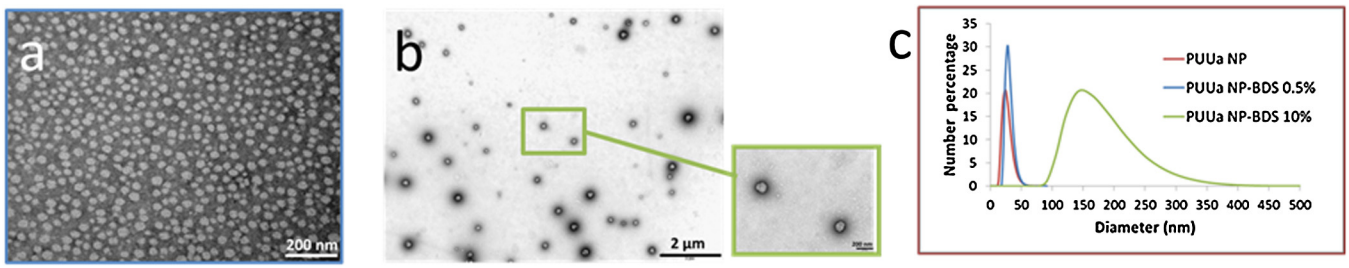


**Fig. 2.** Nanoparticle characterization. (a) TEM micrograph of PUUa NPs-BDS 0.5%. (b) TEM micrograph of PUUa NPs-BDS 10%. (c) DLS plot of hydrodynamic diameters of study formulations.

influenced Amphil and Hyfob self-assembly by hydrophobic interactions. This led to NP sizes of around 170 ± 52 nm (PDI = 0.09), as confirmed by TEM and DLS.

### 3.2. Drug loading (DL) and encapsulation efficiency (EE)

BDS was encapsulated at 0.5 and 10% (*w/w*) in PUUa NPs. As expected, both nanosytems exhibited excellent encapsulation efficiency (above 95%), as quantified by the HPLC calibration method explained in material and methods. A DL of 0.48 ± 0.06% and 9.9 ± 0.1% was achieved respectively. EE was 99.7 ± 0.2% for NP-BDS 0.5% and 99 ± 0.1% for NP-BDS 10%. Importantly, there was no release in the absence of glutathione (data not shown).

### 3.3. Generation of tol-DCs using PUUa NPs-BDS 0.5%

#### 3.3.1. DCs internalize PUUa NPs

In our previous paper, we proved that the encapsulation stability of PUUa NPs was extremely high under *in vivo-like* media and that the hydrophobic cargo was dependent on high glutathione concentration and was delivered intracellularly and not passively diffused extracellularly (Zou et al., 2013; Chen et al., 2008). To first establish whether PUU NPs were internalized by human DCs, we analyzed purified cells incubated with fluorescent labeled DiI-loaded PUUa NPs for 10, 30 and 120 min at both 37 °C and 4 °C. Internalization was measured by flow cytometry. DCs incubated with DiI-loaded PUUa NPs presented the highest ratio of internalization at 120 min at 37 °C, with up to 70 ± 14.4% of DCs positive for DiI staining (Fig. 3a). In contrast, DCs incubated at 4 °C did not internalize the PUUa NPs at 120 min, thereby indicating that PUU NP incorporation is an active phagocytic process (Fig. 3b). Moreover, we used fluorescence microscopy to confirm that PUUa NPs were indeed internalized and not merely bound to the membrane. Most of the NPs-DiI internalized by DCs were located in the cytoplasm and did not co-localize with membrane MHCII staining (Fig. 3c). Furthermore, to demonstrate that PUUa NPs were internalized only by DCs and other phagocytes and not passively incorporated by other immune cells, we incubated total PBMCs with Cadaverine-labeled PUUa NPs. NP internalization was analyzed by flow cytometry in T-lymphocytes (CD3+), B-lymphocytes (CD19+) and monocytes (CD14+). PUUa NPs were internalized efficiently only by CD14+ monocytes, which were mostly dendritic and phagocytic cells (Fig. 1Sa) and not by T- or B-lymphocytes.

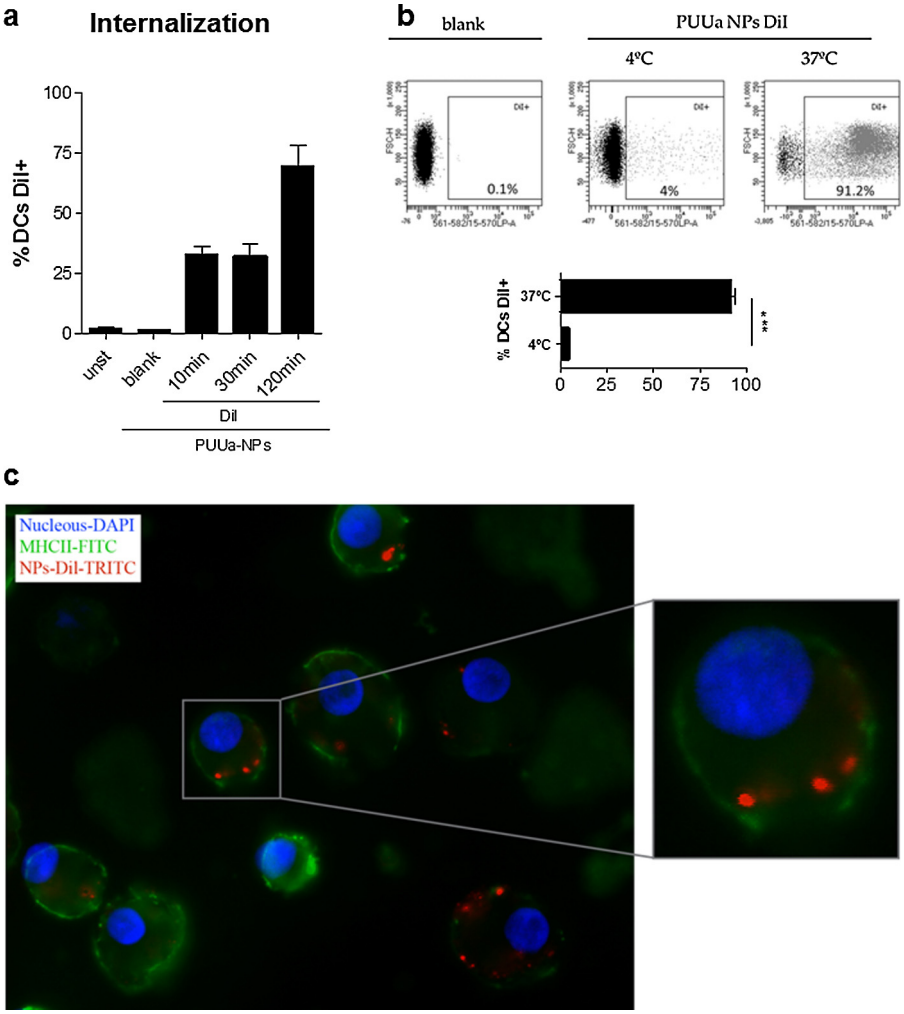


**Fig. 3.** NP internalization by DCs. (a) DCs were incubated with DiI-loaded PUUa NPs for 10, 30 or 120 min, and flow cytometry was performed. Percentage of DiI+ cells is presented as mean ± SD of n = 2 independent experiments. (b) DCs were incubated with DiI-loaded PUUa NPs for 120 min at both 4 °C and 37 °C, and flow cytometry was performed. Percentage of DiI+ cells is presented as mean ± SD of n = 3 independent experiments (c) Fluorescence microscopy images (20×) of DCs incubated with PUUa NPs-DiI for 120 min. Picture shows membrane MHCII-FITC (in green), PUUa NPs-DiI (in red), and nucleus (in blue). (For interpretation of the references to color in this figure legend, the reader is referred to the web version of this article.)

*3.3.2. Incorporation of PUUa NPs-BDS 0.5% efficiently generates tol-DCs*

As shown above, PUUa NPs were efficiently internalized by human DCs. To rule out NP toxicity in human primary cells, we analyzed DC viability after 4 days of co-culture with PUUa NPs-BDS. At the maximum dose (1 μM), these nanoparticles did not affect the viability of the DCs treated, which was over 85% (Fig. 1Sb).

It has been previously described that tol-DCs generated with glucocorticoids are characterized by lower expression of costimulatory molecules in response to stimuli compared to mature DCs. In addition, MERTK was recently described to be upregulated in tol-DCs and may be involved in tolerance induction (Cabezón et al., 2012, 2015). Therefore, we evaluated the generation of tol-DCs using PUUa NPs-BDS 0.5% in comparison to tol-DCs generated with free BDS. To assess the tolerogenic properties of DCs treated with different concentrations of PUUa NPs-BDS 0.5% (0.05, 0.1 and 1 μM) or free BDS (1 μM), we analyzed the expression of costimulatory or inhibitory molecules by flow cytometry and the cytokine secretion profile by ELISA.

In this regard, our results show that PUUa NPs-BDS 0.5% prominently prevented the upregulation of CD80, CD83 and MHCII levels compared to our control of mDCs. In fact, the tolerogenic effect of 0.5% encapsulated BDS at 1.0 μM on DCs phenotype was

Figure 4

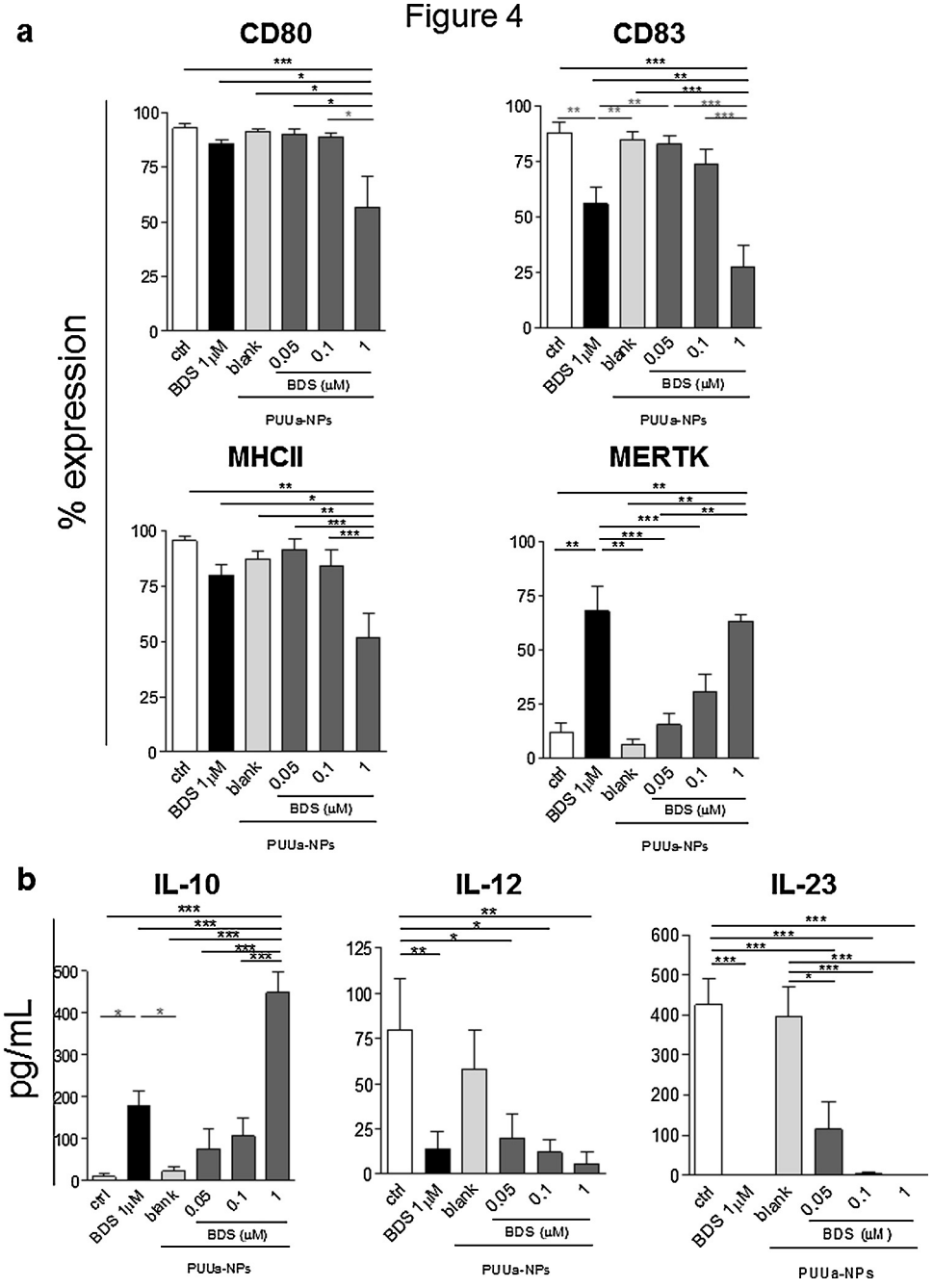


**Fig. 4.** Characterization of tol-DC generation using PUUa NPs-BDS 0.5%. (a) tol-DCs were generated with PUUa NPs-BDS 0.5% at a range of BDS doses (0.05, 0.1 and 1 μM) and compared to soluble BDS (1 μM). Expression of surface costimulatory molecules was analyzed by flow cytometry. Results are presented as the mean ± SD of n = 6 independent experiments. (b) Cytokine production by DCs stimulated with LPS (100 ng/mL) for 24 h. IL-10, IL-12 and IL-23 levels were analyzed in the supernatants of DC culture by ELISA. Results are presented as the mean ± SD of n = 6 independent experiments.

much more powerful than free BDS at the same dose of 1.0 μM (18.8% CD80, 37.6% CD83 and 25.7% MHCII reduction compared to free BDS, respectively) (Fig. 4a). In addition, the tolerogenic tyrosine kinase receptor MERTK was upregulated in tol-DCs and its expression in PUUa NPs-BDS 0.5% treated DCs showed a directly proportional dose-dependent expression effect (Fig. 4a).

Next, we measured cytokine production after DCs stimulation with LPS. DCs treated with either free or encapsulated BDS produced higher levels of IL-10 compared to mDCs. Interestingly, IL-10 production by DCs treated with PUUa NPs-BDS 0.5% 1 μM was remarkably higher (60% more) than that of DCs treated with free BDS at the same concentration (Fig. 4b) (420 ± 120 pg/ml versus 180 ± 88 pg/ml; p = 0.0007). The production of pro-inflammatory cytokines IL-12p70 and IL-23 in response to LPS was efficiently reduced in DCs treated with both free BDS and PUUa NPs-BDS 0.5% compared with control mDCs and mDCs treated with empty PUUa NPs (Fig. 4b).

In addition, we explored how the effect of different BDS loadings in PUUa NPs affected the tolerogenic profile of DCs. In this regard, two different loadings of BDS, either 0.5% or 10% were tested. However, after incubation of both formulations at 1 μM final concentration of BDS we did not observe differences in the modulation of CD83 or Mertk expression in DCs (Fig. 2Sa).

*3.3.3. Kinetics of IL-10 production by Tol-DCs*

As shown in Fig. 4b, the release of BDS inside DCs increased the production of IL-10 by tol-DCs. Therefore, we studied the relationship between the amount of encapsulated BDS and DC anti-inflammatory response by examining IL-10 secretion kinetics. IL-10 was analyzed at 4, 8, 12, 24 and 48 h after addition of LPS to DCs previously incubated with free BDS, PUUa NPs-BDS 0.5%, PUUa NPs-BDS 10% or empty PUUa NPs. While the amount of encapsulated BDS did not influence DC's phenotype (Fig. 2Sa), we did observe variations in IL-10 production by tol-DCs, when generated with PUUa NPs loaded with different amounts of BDS. Interestingly the highest IL-10 production was induced by PUUa NPs-BDS 0.5% at both 24 and 48 h (Fig. 2Sb), whereas BDS at 10% induced a similar pattern of IL-10 production as free BDS.

*3.4. DCs treated with PUUa NPs-BDS 0.5% have a tolerogenic function*

To study the functional consequences of tol-DCs generated by PUUa NPs-BDS 0.5% incubation, we set up a mixed leukocyte response (MLR) – a standard assay for measuring the DC immunogenicity – which consisted of a DC co-culture with allogeneic T-cells. Tol-DCs generated with free BDS or PUUa NPs-BDS 0.5% (1 μM) showed less capacity to induce T-cell proliferation as well as IFNγ production than mDCs or DCs incubated with empty PUUa NPs. In this case, we did not observe statistically significant differences between free and encapsulated BDS (p = 0.33) (Fig. 5), although both the proliferative response and IFNγ production induced by PUUa NPs-BDS 0.5% was numerically lower than that of free BDS.

To confirm that PUUa NPs-BDS 0.5% were effective only when internalized by DCs, naive T-cells were incubated with free or encapsulated BDS, and T-cell proliferation was measured after αCD3αCD28 polyclonal stimulation. Our results corroborated that, in the absence of DCs in the culture, PUUa NPs-BDS 0.5% did not release BDS unspecifically in the medium and thus did not modify T-cell activation due to BDS passive diffusion. In contrast, free BDS significantly reduced IFN-γ production (about 60% decrease) (Fig. 2 Sc).

## 4. Discussion

The present study is the first to address PUUa-NPs as delivery system to target DCs using BDS as an immunosuppressive agent to generate tol-DCs. This innovative delivery system prevented drug release before the internalization of PUUa NPs by phagocytic cells. Interestingly, PUUa NPs did not contain any external surfactant. Moreover, cryoprotectants were not required for lyophilization or redispersion procedures. We propose that is due to the combination of the PEG-like structure of YMER N-120, which retains water molecules, and the structural stability conferred during cross-linking. This process allowed the NP shell to maintain its nanostructure during freeze-drying, thus conserving dangling hydrophilic chains on the surface of the shell (Moyano et al., 2014). These characteristics of drug nanoencapsulation confer a clear

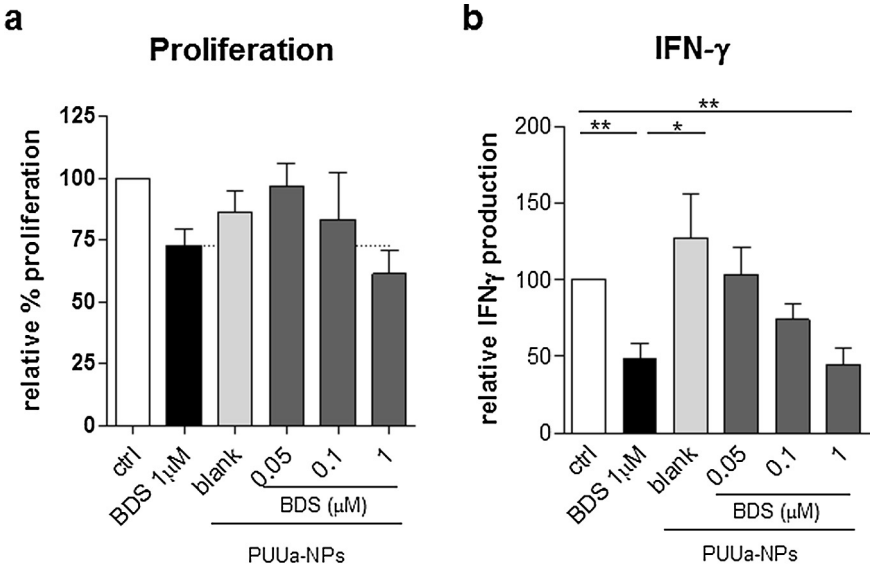


**Fig. 5.** Lymphocyte activation. (a) Mixed lymphocyte reaction (MLR). DCs treated with PUUa NPs-BDS 0.5% using different BDS doses (0.05, 0.1 and 1 μM) and with free BDS 1 μM were co-cultured with allogeneic PBLs for 7 days. Lymphocyte proliferation was measured by incorporation of Tritiated Thymidine. Results have been normalized using the control and are presented as the mean ± SD of n = 5 independent experiments (b) IFN-γ production was analyzed from the supernatant of MLR by ELISA. Results have been normalized using the control are presented as the mean ± SD of n = 5 independent experiments.

advantage for the future translation of this nanosystem to *in vivo* preclinical studies. PUUa NPs were synthesized to be biodegradable upon exposure to intracellular levels of reduced glutathione (GSH). Moreover, their GSH-mediated degradation and release kinetics of encapsulated hydrophobic molecules was fully described previously (Rocas et al., 2015, 2016).

In this study, we evaluate whether PUUa NPs can be used for the selective delivery of drugs to specific immune cells. In particular, primary human DCs are a relevant cell subset to target due to their key role in regulating the immune response. The results shown in this manuscript demonstrate that PUUa NPs-BDS induced tol-DCs from monocyte-derived cells and that these tol-DCs show enhanced tolerogenic properties compared to those treated with free BDS. The treatment with PUUa NPs-BDS prompted the modulation of maturation molecules, downregulated costimulatory receptors, and specially up-regulated MERTK, which has been shown to be clearly involved in controlling T cell proliferation and cytokine production (Cabezón et al., 2015). Furthermore, PUUa NP-BDS treatment significantly increased IL-10 production by DCs, which is essential to induce tolerance.

We hypothesize that the full digestion of PUUa NPs-BDS 0.5% and BDS cytosolic release upon active endocytosis is caused by the endogenous capacity of DCs to degrade internalized pathogens and their high constitutive concentration of reduced GSH compared to other immune cells subsets (Kamide et al., 2011). It is then conceivable to speculate that the encapsulation of BDS provides each DC with high intracellular concentrations of the drug, while DC treatment with the free drug leads to a lower final concentration.

Nanoparticle size is relevant for nanoparticle-cell interactions. In particular, nanoparticles below 50 nm show greater internalization and enhanced therapeutic effects than their counterparts ranging above 100 nm (Reddy et al., 2006; Shang et al., 2014). Normally, drug release quantification studies focus on the physicochemical aspects of this phenomenon and sometimes are not able to mimic neither *in vivo* nor *in vitro* media conditions. Moreover, drug release studies do not provide information about the intracellular fate of such release neither about the therapeutic effect. Thus, we wanted to perform functional studies focusing on how cytokines secretion pattern changed with the size of the delivery system used. Interestingly, we observed that DCs generated with 30 nm PUUa NPs-BDS 0.5% released the largest amounts of IL-10 at 48 h upon exposure to LPS compared to 170 nm PUUa NPs-BDS 10% and free BDS. Such kinetic studies of IL-10 release served us as a more accurate prediction of the therapeutic effect of budesonide upon *in vitro* intracellular release.

In addition, tol-DCs generated from PUUa NPs-BDS 0.5% were less capable to activate allogeneic T-cells proliferation and IFN-γ production by activated T lymphocytes, thus revealing strong functional tolerogenic properties. Moreover, our results indicate that the effect achieved is due to aspecific cargo release on DCs upon internalization of PUUa NPs-BDS 0.5% since PBLs were carefully washed before adding them to the DC co-culture. In this line, we observed that PUUa NPs were only internalized by phagocytic cells when incubated with total PBMCs, further supporting the notion that the drug is not released extracellularly. The incubation of purified naïve T lymphocytes with PUUa NPs-BDS 0.5% during polyclonal activation did not induce any tolerogenic effect measured by cell proliferation and IFN-γ production. In fact, we observed that only free BDS drastically reduced both T-cells proliferation and IFN-γ production due to the lack of cell internalization specificity. These results indicate that in the absence of targeted-DCs (or phagocytic cells), the PUUa NPs have not effect in other cells like T lymphocytes.

In this manuscript we describe PUUa NPs as an innovative, interesting and highly cell-subset specific delivery system. The advantage of this approach is that encapsulated drugs or alternatively adjuvants and/or antigens, only have an effect on those cells that are targeted to, thereby preventing systemic inhibition or activation and off-target toxicities, and conversely, that DCs loaded with antigens are those cells that also simultaneously receive the tolerogenic or immunogenic agent.

## 5. Conclusions

In summary, here we report that self-stratified PUUa NPs boost the effect of lipophilic corticosteroids in human DCs. Specifically; PUUa NPs-BDS 0.5% exhibited strong encapsulation capacity, thereby allowing the efficient internalization of the drug-loaded nanosystems, as observed by flow cytometry and fluorescence microscopy. Moreover, this internalization and drug release translated into a more potent tolerogenic profile of DCs compared to the DCs obtained with free BDS treatment. Furthermore, PUUa NPs exhibited a selective targeting to DCs and their precursors without affecting other immune cell subsets. This observation therefore provides robust evidence of the potential of PUUa NPs as a selective drug delivery system for the treatment of autoimmune diseases. More research is currently underway to actively target DCs in *in vivo* animal models of human diseases, such as autoimmune or chronic inflammatory conditions. Interestingly the encapsulation of alternative agents to either stimulate (adjuvants) or inhibit the immune response, in combination with defined disease-associated antigens (or synthetic peptides), will increase the possibility of designing more precise therapies to target human DCs for immune-mediated diseases.

## Funding body agreements and policies

This research was supported by Grant SAF 2009-07272 from the Ministerio de Ciencia e Innovación, Grant TRA-097 from the Ministerio de Sanidad y Politica Social, Grant FIS PI13/01585 from the Instituto Carlos III (to D.B.-R.). D.B.-R is also supported by CIBERehd. We also gratefully acknowledge MICINN and ERDF (IPT-090000-2010-0001), CICYT (CTQ2012-30930), and the Generalitat de Catalunya (2014 SGR 137). Images were taken and adapted from Servier Medical Art.

## Conflict of interest

The Authors declare that there are no conflicts of interests.

## Contributors

All authors have approved the final article.

## Authorship

G.F.-G. and P.R designed and performed the research, analyzed and interpreted data, and wrote the manuscript. R.C. and C.E. performed the research. J.R., J.P., and F.A. designed the research and interpreted data. D.B.-R. designed the research, analyzed and interpreted data, and wrote the manuscript.

## Appendix A. Supplementary data

Supplementary data associated with this article can be found, in the online version, at http://dx.doi.org/10.1016/j.ijpharm.2016.07.056.

## References


Ali, H., Weigmann, B., Neurath, M.F., Collnot, E.M., Windbergs, M., Lehr, C.M., 2014. Budesonide loaded nanoparticles with pH-sensitive coating for improved mucosal targeting in mouse models of inflammatory bowel diseases. J. Control. Release 183, 167–177. doi:http://dx.doi.org/10.1016/j.jconrel.2014.03.039.

Amoozgar, Z., Goldberg, M.S., 2015. Targeting myeloid cells using nanoparticles to improve cancer immunotherapy. Adv. Drug Deliv. Rev. 91, 38–51. doi:http://dx.doi.org/10.1016/j.addr.2014.09.007.

Anguille, S., Smits, E.L., Lion, E., van Tendeloo, V.F., Berneman, Z.N., 2014. Clinical use of dendritic cells for cancer therapy. Lancet Oncol. 15, e257–e267. doi:http://dx.doi.org/10.1016/S1470-2045(13)70585-0.

Banchereau, J., Steinman, R.M., 1998. Dendritic cells and the control of immunity. Nature 392, 245–252. doi:http://dx.doi.org/10.1038/32588.

Banchereau, J., Briere, F., Caux, C., Davoust, J., Lebecque, S., Liu, Y., et al., 2000. Immunobiology of dendritic cells. Annu. Rev. Immunol. 18, 767–811. doi:http://dx.doi.org/10.1146/annurev.immunol.18.1.767.

Beloqui, A., Coco, R., Alhouayek, M., Solinís, M.Á., Rodríguez-Gascón, A., Muccioli, G. G., et al., 2013. Budesonide-loaded nanostructured lipid carriers reduce inflammation in murine DSS-induced colitis. Int. J. Pharm. 454, 775–783. doi:http://dx.doi.org/10.1016/j.ijpharm.2013.05.017.

Benham, H., Nel, H.J., Law, S.C., Mehdi, A.M., Street, S., Ramnoruth, N., et al., 2015. Citrullinated peptide dendritic cell immunotherapy in HLA risk genotype-positive rheumatoid arthritis patients. Sci. Transl. Med. 7 doi:http://dx.doi.org/10.1126/scitranslmed.aaa9301 290ra87–290ra87.

Butterfield, L.H., 2013. Dendritic cells in cancer immunotherapy clinical trials: are we making progress? Front. Immunol. 4, 454. doi:http://dx.doi.org/10.3389/fimmu.2013.00454.

Cabezón, R., Benítez-Ribas, D., 2013. Therapeutic potential of tolerogenic dendritic cells in IBD: from animal models to clinical application. Clin. Dev. Immunol. 2013 (789814) doi:http://dx.doi.org/10.1155/2013/789814.

Cabezón, R., Ricart, E., España, C., Panés, J., Benitez-Ribas, D., 2012. Gram-negative enterobacteria induce tolerogenic maturation in dexamethasone conditioned dendritic cells. PLoS One 7, e52456. doi:http://dx.doi.org/10.1371/journal.pone.0052456.

Cabezón, R., Carrera-Silva, E.A., Flórez-Grau, G., Errasti, A.E., Calderón-Gómez, E., Lozano, J.J., et al., 2015. MERTK as negative regulator of human T cell activation. J. Leukoc. Biol. doi:http://dx.doi.org/10.1189/jlb.3A0714-334R jlb.3A0714–334R–.

Chen, H., Kim, S., Li, L., Wang, S., Park, K., Cheng, J.-X., 2008. Release of hydrophobic molecules from polymer micelles into cell membranes revealed by Förster resonance energy transfer imaging. Proc. Natl. Acad. Sci. 105, 6596–6601. doi:http://dx.doi.org/10.1073/pnas.0707046105.

Cheung, A.S., Mooney, D.J., 2015. Engineered materials for cancer immunotherapy. Nano Today doi:http://dx.doi.org/10.1016/j.nantod.2015.06.007.

Cho, N.-H., Cheong, T.-C., Min, J.H., Wu, J.H., Lee, S.J., Kim, D., et al., 2011. A multifunctional core-shell nanoparticle for dendritic cell-based cancer immunotherapy. Nat. Nanotechnol. 6, 675–682. doi:http://dx.doi.org/10.1038/nnano.2011.149.

Clemitson, I.R., 2008. Castable Polyurethane Elastomers. CRC Press.

Collin, M., McGovern, N., Haniffa, M., 2013. Human dendritic cell subsets. Immunology 140, 22–30. doi:http://dx.doi.org/10.1111/imm.12117.

De Fuente, M., Langer, R., Alonso, M.J., 2014. Nano Oncologicals doi:http://dx.doi.org/10.1007/978-3-319-08084-0.

Fang, R.H., Hu, C.-M.J., Luk, B.T., Gao, W., Copp, J.A., Tai, Y., et al., 2014. Cancer cell membrane-Coated nanoparticles for anticancer vaccination and drug delivery. Nano Lett. 14, 2181–2188. doi:http://dx.doi.org/10.1021/nl500618u.

García-González, P., Morales, R., Hoyos, L., Maggi, J., Campos, J., Pesce, B., et al., 2013. A short protocol using dexamethasone and monophosphoryl lipid A generates tolerogenic dendritic cells that display a potent migratory capacity to lymphoid chemokines. J. Transl. Med. 11, 128. doi:http://dx.doi.org/10.1186/1479-5876-11-128.

Gharagozloo, M., Majewski, S., Foldvari, M., 2015. Therapeutic applications of nanomedicine in autoimmune diseases: from immunosuppression to tolerance induction. Nanomed. Nanotechnol. Biol. Med. 11, 1003–1018. doi:http://dx.doi.org/10.1016/j.nano.2014.12.003.

Hackstein, H., Thomson, A.W., 2004. Dendritic cells: emerging pharmacological targets of immunosuppressive drugs. Nat. Rev. Immunol. 4, 24–34. doi:http://dx.doi.org/10.1038/nri1256.

Hu, J., Wan, Y., 2011. Tolerogenic dendritic cells and their potential applications. Immunology 132, 307–314. doi:http://dx.doi.org/10.1111/j.1365-2567.2010.03396.x.

Jauregui-Amezaga, A., Cabezón, R., Ramírez-Morros, A., España, C., Rimola, J., Bru, C., et al., 2015. Intraperitoneal administration of autologous tolerogenic dendritic cells for refractory crohn's disease: a phase I study. J. Crohns. Colitis doi:http://dx.doi.org/10.1093/ecco-jcc/jjv144.

Kalantari, T., Kamali-Sarvestani, E., Ciric, B., Karimi, M.H., Kalantari, M., Faridar, A., et al., 2011. Generation of immunogenic and tolerogenic clinical-grade dendritic cells. Immunol. Res. 51, 153–160. doi:http://dx.doi.org/10.1007/s12026-011-8255-5.

Kamide, Y., Utsugi, M., Dobashi, K., Ono, A., Ishizuka, T., Hisada, T., et al., 2011. Intracellular glutathione redox status in human dendritic cells regulates IL-27 production and T-cell polarization. Allergy 66, 1183–1192 (10.1111/j.1398-9995.2011.02611.x).

Kirkwood, J.M., Butterfield, L.H., Tarhini, A.A., Zarour, H., Kalinski, P., Ferrone, S., 2012. Immunotherapy of cancer in 2012. CA Cancer J. Clin. 62, 309–335. doi:http://dx.doi.org/10.3322/caac.20132.

Leonard, F., Ali, H., Collnot, E.M., Crielaard, B.J., Lammers, T., Storm, G., et al., 2012. Screening of budesonide nanoformulations for treatment of inflammatory bowel disease in an inflamed 3D cell-culture model. ALTEX 29, 275–285.

Moyano, D.F., Ray, M., Rotello, V.M., 2014. Nanoparticle—protein interactions: water is the key, 39 1069–1073. 10.1557/mrs.2014.255.

Naranjo-Gómez, M., Raïch-Regué, D., Oñate, C., Grau-López, L., Ramo-Tello, C., Pujol-Borrell, R., et al., 2011. Comparative study of clinical grade human tolerogenic dendritic cells. J. Transl. Med. 9, 89. doi:http://dx.doi.org/10.1186/1479-5876-9-89.

Park, Y.-M., Lee, S.J., Kim, Y.S., Lee, M.H., Cha, G.S., Jung, I.D., et al., 2013. Nanoparticle-based vaccine delivery for cancer immunotherapy. Immune Netw. 13, 177–183. doi:http://dx.doi.org/10.4110/in.2013.13.5.177.

Prabhakar, A., Chattopadhyay, D.K., Jagadeesh, B., Raju, K.V.S.N., 2005. Structural investigations of polypropylene glycol (PPG) and isophorone diisocyanate (IPDI)-based polyurethane prepolymer by 1D and 2D NMR spectroscopy. J. Polym. Sci. Part A Polym. Chem. 43, 1196–1209. doi:http://dx.doi.org/10.1002/pola.20583.

Pulendran, B., Tang, H., Manicassamy, S., 2010. Programming dendritic cells to induce T(H)2 and tolerogenic responses. Nat. Immunol. 11, 647–655. doi:http://dx.doi.org/10.1038/ni.1894.

Reddy, S.T., Rehor, A., Schmoekel, H.G., Hubbell, J.A., Swartz, M.A., 2006. In vivo targeting of dendritic cells in lymph nodes with poly(propylene sulfide) nanoparticles. J. Control. Release 112, 26–34. doi:http://dx.doi.org/10.1016/j.jconrel.2006.01.006.

Rocas Alonso, P., Rocas Sorolla, J., 2014. Method for producing a microencapsulate and corresponding reactive amphiphilic compound, microencapsulate and composition, WO2014114838A3 Ecopol Tech S.L.

Rocas, P., Fernández, Y., Schwartz, S., Abasolo, I., Rocas, J., Albericio, F., 2015. Multifunctionalized polyurethane–polyurea nanoparticles: hydrophobically driven self-stratification at the o/w interface modulates encapsulation stability. J. Mater. Chem. B 3, 7604–7613. doi:http://dx.doi.org/10.1039/C5TB01345C.

Rocas, P., Fernández, Y., García-Aranda, N., Foradada, L., Calvo, P., Avilés, P., et al., 2016. Improved pharmacokinetic profile of lipophilic anti-cancer drugs using $\alpha\nu\beta3$-targeted polyurethane-polyurea nanoparticles (Submitted elsewhere).

Shang, L., Nienhaus, K., Nienhaus, G.U., 2014. Engineered nanoparticles interacting with cells: size matters. J. Nanobiotechnol. 12, 5. doi:http://dx.doi.org/10.1186/1477-3155-12-5.

Shao, K., Singha, S., Clemente-Casares, X., Tsai, S., Yang, Y., Santamaria, P., 2014. Nanoparticle-Based immunotherapy for cancer. ACS Nano 9, 16–30. doi:http://dx.doi.org/10.1021/nn5062029.

Siddique, M.I., Katas, H., Iqbal Mohd Amin, M.C., Ng, S.-F., Zulfakar, M.H., Buang, F., et al., 2015. Minimization of local and systemic adverse effects of topical glucocorticoids by nanoencapsulation: in vivo safety of hydrocortisone-hydroxytyrosol loaded chitosan nanoparticles. J. Pharm. Sci. 104, 4276–4286. doi:http://dx.doi.org/10.1002/jps.24666.

Steinman, R.M., Banchereau, J., 2007. Taking dendritic cells into medicine. Nature 449, 419–426. doi:http://dx.doi.org/10.1038/nature06175.

Steinman, R.M., Hawiger, D., Nussenzweig, M.C., 2003. Tolerogenic dendritic cells. Annu. Rev. Immunol. 21, 685–711. doi:http://dx.doi.org/10.1146/annurev.immunol.21.120601.141040.

Suwandi, J.S., Toes, R.E.M., Nikolic, T., Roep, B.O., 2016. Inducing tissue specific tolerance in autoimmune disease with tolerogenic dendritic cells. Clin. Exp. Rheumatol. 33, 97–103.

Tacken, P.J., de Vries, I.J.M., Torensma, R., Figdor, C.G., 2007. Dendritic-cell immunotherapy: from ex vivo loading to in vivo targeting. Nat. Rev. Immunol. 7, 790–802. doi:http://dx.doi.org/10.1038/nri2173.

Van Kooten, C., Stax, A.S., Woltman, A.M., Gelderman, K.A., 2009. The use of dexamethasone in the induction of tolerogenic DCs. Handb. Exp. Pharmacol. 188, 233–249. doi:http://dx.doi.org/10.1007/978-3-540-71029-5_11.

Zheng, G., Zhong, S., Geng, Y., Munirathinam, G., Cha, I., Reardon, C., et al., 2013. Dexamethasone promotes tolerance in vivo by enriching CD11clo CD40lo tolerogenic macrophages. Eur. J. Immunol. 43, 219–227. doi:http://dx.doi.org/10.1002/eji.201242468.

Zou, P., Chen, H., Paholak, H.J., Sun, D., 2013. Noninvasive fluorescence resonance energy transfer imaging of in vivo premature drug release from polymeric nanoparticles. Mol. Pharm. 10, 4185–4194. doi:http://dx.doi.org/10.1021/mp4002393.